Predicting Seabed Burial of Cylinders by Wave-Induced Scour: Application to the Sandy Inner Shelf Off Florida and Massachusetts

Arthur C. Trembanis, Carl T. Friedrichs, Michael D. Richardson, Peter Traykovski, Peter A. Howd,
Paul A. Elmore, and Thomas F. Wever

***Abstract*—A simple parameterized model for wave-induced burial of mine-like cylinders as a function of grain-size, time-varying, wave orbital velocity and mine diameter was implemented and assessed against results from inert instrumented mines placed off the Indian Rocks Beach (IRB, FL), and off the Martha's Vineyard Coastal Observatory (MVCO, Edgartown, MA). The steady flow scour parameters provided by Whitehouse (1998) for self-settling cylinders worked well for predicting burial by depth below the ambient seabed for O (0.5 m) diameter mines in fine sand at both sites. By including or excluding scour pit infilling, a range of percent burial by surface area was predicted that was also consistent with observations. Rapid scour pit infilling was often seen at MVCO but never at IRB, suggesting that the environmental presence of fine sediment plays a key role in promoting infilling. Overprediction of mine scour in coarse sand was corrected by assuming a mine within a field of large ripples buries only until it generates no more turbulence than that produced by surrounding bedforms. The feasibility of using a regional wave model to predict mine burial in both hindcast and real-time forecast mode was tested using the National Oceanic and Atmospheric Administration (NOAA, Washington, DC) WaveWatch 3 (WW3) model. Hindcast waves were adequate for useful operational forcing of mine burial predictions, but five-day wave forecasts introduced large errors. This investigation was part of a larger effort to develop simple yet reliable predictions of mine burial suitable for addressing the operational needs of the U.S. Navy.**

***Index Terms*—Heterogeneous sediment, inner continental shelf, mine burial, real-time forecasts, scour modeling.**

I. INTRODUCTION

PROVIDING meaningful estimates of the degree of settling and/or exposure of seabed mines is of critical concern in mine countermeasure efforts [1]–[3]. A major goal of the mine burial prediction (MBP) program sponsored by the U.S. Office of Naval Research (ONR, Arlington, VA) is to provide the operational U.S. Navy with a prototype model for predicting subsequent (postseabed impact) mine burial that works with a known and useful degree of accuracy in regions of strategic interest, initially defined as sandy inner shelves dominated by waves. To be useful under real-world conditions, such a model must be reasonably accurate and reliable but also numerically executable in a practical, straightforward manner. Thus, the model must parameterize the complicated and computationally intense details of localized scour. In response to the aforementioned needs, the aim of this paper is to demonstrate the practical utility of predicting scour-related mine burial using a simple parameterized model forced by readily available wave forecasts. To this end, a combined field and modeling study of scour related mine burial was conducted off the Indian Rocks Beach (IRB, FL) [4]–[6] and near the Martha's Vineyard Coastal Observatory (MVCO, Edgartown, MA) [7]–[9].

Scour is the morphodynamic response of a moveable seabed to the presence of an object that disturbs the local fluid flow [10]. The presence of an object on the seabed produces local flow acceleration, increasing bed shear stress and turbulence as structured vortices develop, driving a flux of sediment away from the object and lowering the surrounding bed. Scour is important to the fate of a variety of marine objects including bridge piers, dock pilings, breakwaters, oil platforms, offshore pipelines, marine artifacts, and naval mines [11]–[13].

Scour can be classified both in terms of spatial extent and hydrodynamics. The two main spatial classes of scour are "local scour," which is near the object (on the order of meters) and "global scour," which is manifest as wide depressions around large or multiple objects (on the order of tens of meters) [11]. In terms of hydrodynamic intensity, scour is classified as either *clear water* when the ambient flow (bed shear stress) is below threshold velocity or *live bed* when ambient flow is above threshold velocity and the entire bed is active. In the former, the amplification of flow around the object induces transport locally but elsewhere the bed is inactive. In the latter case, sediment is

Manuscript received April 29, 2005; revised October 3, 2005; accepted February 21, 2006. This work was supported by the grants from the U.S. Office of Naval Research Marine Geosciences Program. The work of A. C. Trembanis was supported by the USGS/WHOI Postdoctoral Fellowship.

Guest Editor: R. H. Wilkens.

A. C. Trembanis is with the Coastal Sediments Hydrodynamics and Engineering Laboratory (CSHEL), Department of Geology, University of Delaware, Newark, DE 19716 USA and with the Virginia Institute of Marine Science, Gloucester Point, VA 23062 USA (e-mail: art@udel.edu).

C. T. Friedrichs is with the College of William and Mary, Virginia Institute of Marine Science, Gloucester Point, VA 23062 USA.

M. D. Richardson and P. A. Elmore are with the U.S. Naval Research Laboratory, Stennis Space Center, MS 39529 USA.

P. Traykovski is with the Applied Ocean Physics and Engineering Department, Woods Hole Oceanographic Institution, Woods Hole, MA 02543 USA.

P. A. Howd is with the Center for Coastal and Watershed Studies, U.S. Geological Survey (USGS), St. Petersburg, FL 33701-4846 USA.

T. F. Wever is with the Forschungsanstalt der Bundeswehr für Wasserschall und Geophysik, Kiel 24148, Germany (e-mail: ThomasWever@bwb.org).

Color versions of one or more of the figures in this paper are available online at http://ieeexplore.ieee.org.

Digital Object Identifier 10.1109/JOE.2007.890958

being transported by flow everywhere, especially near the object where turbulence and bed shear stress are enhanced. In this paper, local scour associated with free-settling cylindrical mines is considered.

The paper is organized in the following manner. In Section II, a simple parameterized model for burial of cylindrical objects by wave-induced scour is presented based on well-established engineering equations for seabed scour. In Section III, the scour burial model is calibrated using published mine burial observations collected early in the ONR MBP program offshore Martha's Vineyard, MA. Next, a proof-of-concept real-time mine burial forecasting exercise is presented for the MBP site off IRB, forced by readily available wave and wind forecasts in Section IV. In Section V, observed and hindcast waves are used to force the mine burial model to test its performance against observations of mine burial in fine sand provided by instrumented mines and tripods at both field sites. In Section VI, the issue of scour limitation in coarse sand by bedforms is briefly discussed. Finally, a 2-D web-based interactive model for scour-induced mine burial is described in Section VII that allows end users to explore the model's parameter space in the context of the field experiments at both spatially heterogeneous test sites.

II. SCOUR MODEL

Extensive laboratory and occasional field research has been carried out over the last 30 years in an effort to meaningfully estimate the rate and depth of scour associated with a host of marine structures. The present modeling approach applied and built upon the well-established research of scour around seabed objects as developed in the engineering literature [11], [12], [14], and [15]. Laboratory and field observations have shown that under constant hydrodynamic forcing, the initial rate of scour around seabed objects in sand proceeds rapidly and then decreases as the depth of scour approaches an equilibrium depth for a given intensity of fluid flow given by

$$S(t) = S_{\text{eq}}\left[1 - \exp(-t/T_x)^{P_m}\right] \tag{1}$$

where S_{eq} is the equilibrium scour depth relative to the undisturbed far-field bed, t is instantaneous time, T_x is the characteristic time scale of the scour process, and P_m is a fitting coefficient of O (1), which depends mainly on the object's geometry.

Consistent with recent engineering texts on scour around marine structures [11], [12], we treat the characteristic time scale of scour as an empirical function of the skin-friction Shields parameter just outside the object's influence, normalized by dimensional parameters associated with the problem, namely object diameter (D), acceleration of gravity (g), specific gravity of sand (s), and median sand grain size (d)

$$T_x = F(\theta)D^2\left[g(s-1)d^3\right]^{-1/2}. \tag{2}$$

The far-field Shields parameter is given by

$$\theta = \frac{0.5 f_w U_b^2}{gd(s-1)} \tag{3}$$

where f_w is the wave friction factor. The Shields parameter θ is a fundamental dimensionless parameter that compares the drag force tending to lift a sediment grain to the gravity force tending to keep it still. It is well known that functions of θ predict both initiation of grain motion and the intensity of bedload transport for sand [10]. For scour around pipelines, Sumer and Fredsøe [12] found that (2) applies well for either steady currents or waves without considering wave period, despite the fact that (3) depends on the frequency of oscillatory flow.

Whitehouse [11] applied (1) and (2) to short free settling cylinders under steady, unidirectional flow and found

$$F(\theta) = 0.095\,\theta^{-2.02}, \quad P_m = 0.6, \quad \text{and} \quad S_{\text{eq}} = 0, \quad \text{for } (\theta/\theta_{cr})^{1/2} < 0.75 \tag{4a}$$

$$S_{\text{eq}} = 1.15\,D\left(2(\theta/\theta_{cr})^{1/2} - 1.5\right), \quad \text{for } 0.75 \le (\theta/\theta_{cr})^{1/2} < 1.25 \tag{4b}$$

$$S_{\text{eq}} = 1.15\,D, \quad \text{for } (\theta/\theta_{cr})^{1/2} \ge 1.25. \tag{4c}$$

Although (4a)–(4c) were calibrated by Whitehouse [11] for steady rather than oscillatory flow, they are the only published equations for burial of free settling cylinders consistent with the time-scale equation given by (2) so here we explore their wider applicability. The present analysis is limited in part because we rely upon the same diameter/length ratio and object density as considered by Whitehouse [11].

It is straightforward to apply (4) to oscillatory flow if one assumes that θ represents the Shields parameter due to the peak stress due to waves plus currents. However, previous studies [11], [12], [15] have found that S_{eq} for seabed objects decreases monotonically with decreasing Keulegan–Carpenter number KC $= U_b T/D$, where U_b is the near-bottom wave orbital velocity in meters per second, T is the wave period in seconds, and D is the object diameter in meters. This finding is presumably because the streamwise size of scour-inducing vortices eventually decreases as the duration of the flow in each direction decreases. A goal of this paper is to determine whether (2) can be reasonably applied to cylindrical mine-like objects exposed to waves characteristic of sandy inner shelves.

One of the key metrics pertaining to the physical attitude of a mine on the seafloor that is of particular interest to Naval operations is the depth of the mine relative to the undisturbed far-field seabed. Observations of scour burial by waves indicates that rocking of a cylindrical mine by current or wave action causes the mine to eventually produce a failure of the supporting soil and/or slide down into its own scour pit such that the depth of the base of the mine below the ambient seabed is roughly equivalent to the greatest depth $(S_{\max})$ that the scour pit has reached up to that point in time [2], [7], [16]. Thus, the maximum percent burial by depth relative to the seabed is expressed by

$$\%\text{Burial}_{\text{depth}} = 100\left(\frac{S_{\max}}{D}\right) \tag{5}$$

where D is the diameter of the mine (Fig. 1).

In applying (1)–(5), the instantaneous scour pit depth S is unambiguous as long as the far-field bed stress (represented via θ) remains constant or increases with time. Then, S is always

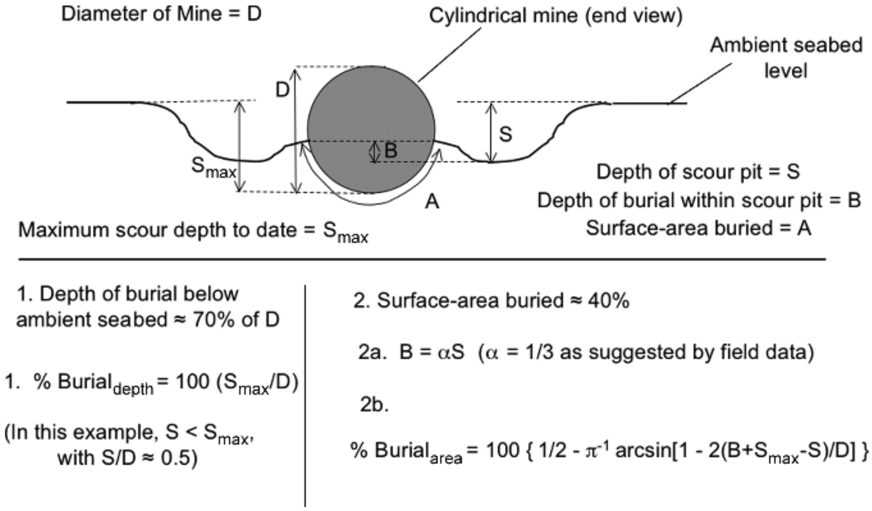

Fig. 1. Diagram of mine burial state in terms of 1) burial by depth below ambient seabed and 2) burial by surface area coverage.

equal to $S_{\max}$. The solution procedure at a new time step $n+1$ is to first use (3) to calculate $\theta(n+1)$ and then solve for $T_x(n+1)$ using (2). Next, (1) is inverted to calculate the effective value of t that corresponds to $T_x(n+1)$ using $S(n)$. Finally, $S(n+1)$ is calculated by stepping forward to $t+\Delta t$ in (1). However, if θ rapidly decreases such that $S_{\text{eq}}(n+1)$ for the new $\theta(n+1)$ is less than $S(n)$ from the previous time step, then the expected behavior of the scour pit as predicted by these functions is less clear.

The two extreme behavioral cases for $S_{\text{eq}}(n+1) < S(n)$ are as follows: 1) $S(n+1)$ stays equal to $S_{\max}$ (i.e., a relict scour pit with no infilling) or 2) $S(n+1)$ immediately decreases to $S_{\text{eq}}(n+1)$ (i.e., an equilibrium scour pit with instantaneous infilling to the new shallower scour depth). Each of these behaviors is straightforward to implement and our model was written with an “on–off” switch to include or exclude scour pit infilling. This approach provides an envelope of instantaneous burial estimates. An aim of future work is to parameterize intermediate cases where scour pits may diffusively decay with time back toward a shallower $S_{\text{eq}}(n+1)$. This binary on–off approach to address the issue of scour pit infilling seems reasonable given the observations that infilling quite often operates only a portion of the time during a deployment record. Since there is presently no clear way to know *a priori* whether or when infilling will operate, turning infilling either always on or always off makes it possible to bracket the end-member possibilities.

A second important metric of mine burial particularly of interest to mine countermeasure operations is the amount of the mine covered by sediment or burial by surface area. It is fairly easy to envision real-world conditions where one or the other of these two principle factors, burial by depth or burial by surface area, would prove most relevant to Naval operations. Consider, for example, a mine resting within a broad scour pit such that the top of the mine is flush with the far-field seafloor but the mine itself remains partly uncovered by sediment. Such a mine potentially would remain a viable weapon but might be difficult to detect with low grazing angle acoustic sensor systems. Detection would ultimately be a function of sensor detection angle as well as sonar penetration depth.

Mine surface area burial is related to, but distinct from, depth of scour. In fact, there is no established theory relating scour pit depth to depth of burial within the scour pit (B). A simple place to start was to assume a simple proportionality such that the average elevation of the sand partially covering the mine within the scour pit (B) was some fixed fraction of the depth of the deepest part of the scour pit (S)

$$B = \alpha S, \qquad \text{where} \quad 0 < \alpha < 1. \tag{6}$$

Assuming the surface area of a cylindrical mine is dominated by its long sides or, more practically, when considering cases where burial sensors on instrumented mines are only on the sides of the mine or when burial on the ends of the mine is negligible [17], then the ends of the mines can be ignored and the rest of the calculation for surface area burial follows from geometry (Fig. 1)

$$\%\text{Burial}_{\text{area}} = 100\left[1/2 - \pi^{-1}\arcsin(1 - 2(B + S_{\max} - S)/D)\right]. \tag{7}$$

In the example illustrated in Fig. 1, $\alpha \approx 1/3$, the mine is approximately 70% buried by depth and ~40% buried by surface area.

III. Field Observations and Scour Forecast Model Calibration

As part of the larger ONR MBP, mine burial experiments were conducted on fine and coarse sandy sediments in ~12-m water depth, 1 km off Martha’s Vineyard, near the MVCO [7]–[9] and in ~12-m water depth, 10 km off IRB [5], [6], [17]. Experimental sites (Fig. 2) were chosen by MBP investigators based on extensive acoustic surveys (sidescan sonar, chirp seismic, and multibeam bathymetry) and sediment samples. Sand suspension at the inner shelf sites at both locations is dominated by waves [7], [18]. Mean currents at each site are primarily tidal with velocities generally below 0.2 m/s. The seabed at both field sites is characterized by closely situated patches of alternating fine and coarse sand associated with ripple scour depressions [19], [20].

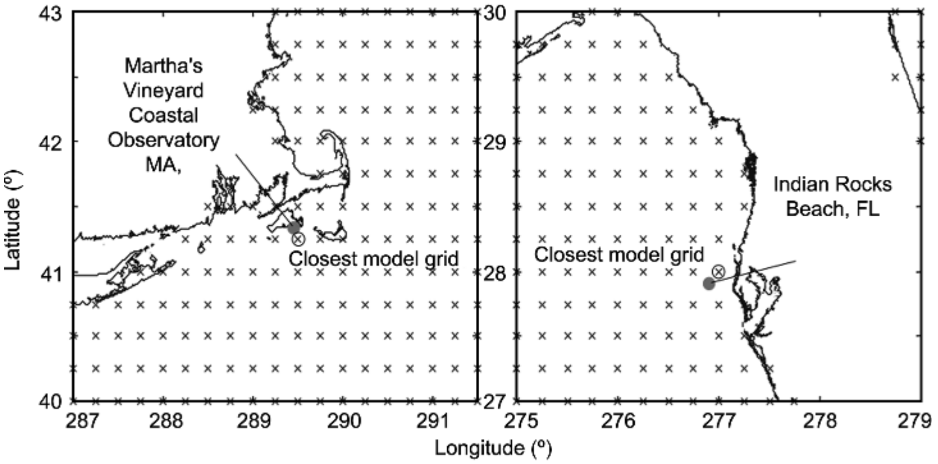

(a) (b)

Fig. 2. Maps of experimental field sites off (a) Martha's Vineyard and (b) IRB along with the locations of WW3 grid cells (Xs). Latitude is in degrees north of the equator. Longitude is in degrees east of the prime meridian.

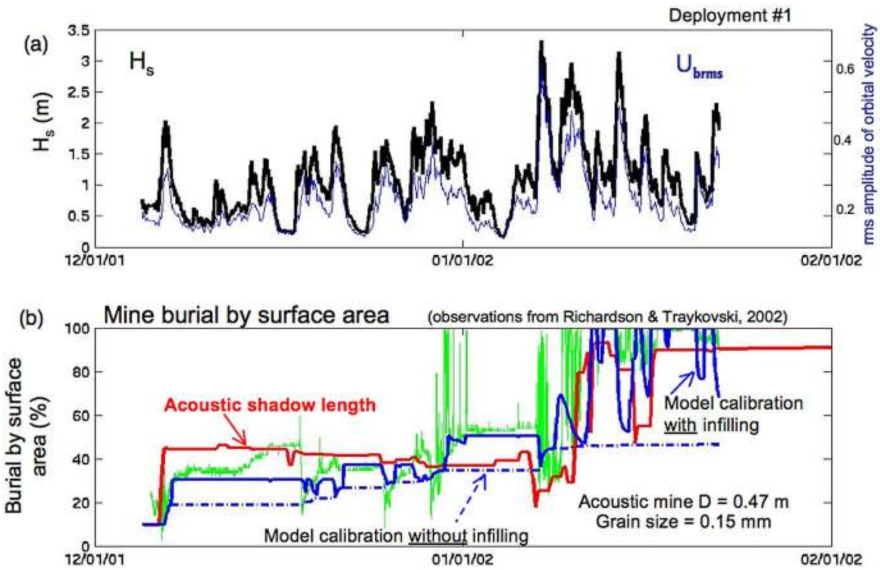

Fig. 3. Calibration of scour model with data from initial Martha's Vineyard Coastal Observatory Deployment (MVCO 1). (a) Observed significant waveheight (thick line) and rms amplitude of near-bed velocity U_b (thin line). (b) Comparison of observed burial by surface area (thick red line is sonar shadow length estimate and thin green line is from optical sensors) to model calibration (thick blue line), either with scour pit infilling (solid line) or without infilling (dashed line). [In grayscale version of panel (b), red and green lines appear gray and blue lines appear black.]

Inert optical and acoustic instrumented mines were deployed off the Florida site during winter 2003 and periodically off Martha's Vineyard between 2001 and 2004. Optical or acoustic sensors mounted around the periphery of the mines allowed measurement of the percent burial by surface area (percent surface area covered with sediment) and helped determine scour pit dimensions [4], [7], [8]. Acoustic mines were also equipped with internal pressure sensors, which helped determine burial by depth beneath the ambient seafloor. For acoustic mines, burial by depth was determined by lowpass filtering of the pressure sensor data from instrumented mines and comparing the record to the stationary pressure data from nearby nonsettling platforms [4], [5], [8], [9]. Additional detailed physical characteristics and instrumentation parameters of the mine-like objects used in these studies can be found in [3] and [21]. Characteristics critical to the present modeling effort have been included in the text and accompanying figures.

A specific goal of this part of the ONR MBP program was to provide proof-of-concept forecasts of mine burial during ongoing field experiments at Martha's Vineyard and IRB. Thus, available results from the initial two instrumented mine deployments [7], [9] were used to calibrate the mine burial model for use in later forecasts. Direct observations of the root mean square (rms) amplitude of near-bed rms wave orbital velocity (U_b) for this first field experiment were available from a current meter deployed 100 m from the instrumented mine [7] and were utilized to calibrate the scour model. All of the scour model parameters in (1)–(4) were kept equal to the values provided in [11]. In our initial implementation, that left the following two unconstrained parameters: 1) the factor relating scour pit depth to partial burial α and 2) the appropriate choice for the friction factor f_w.

For the calibration case, constant best-fit values for α and f_w were selected. Fig. 3 displays a comparison of observed and

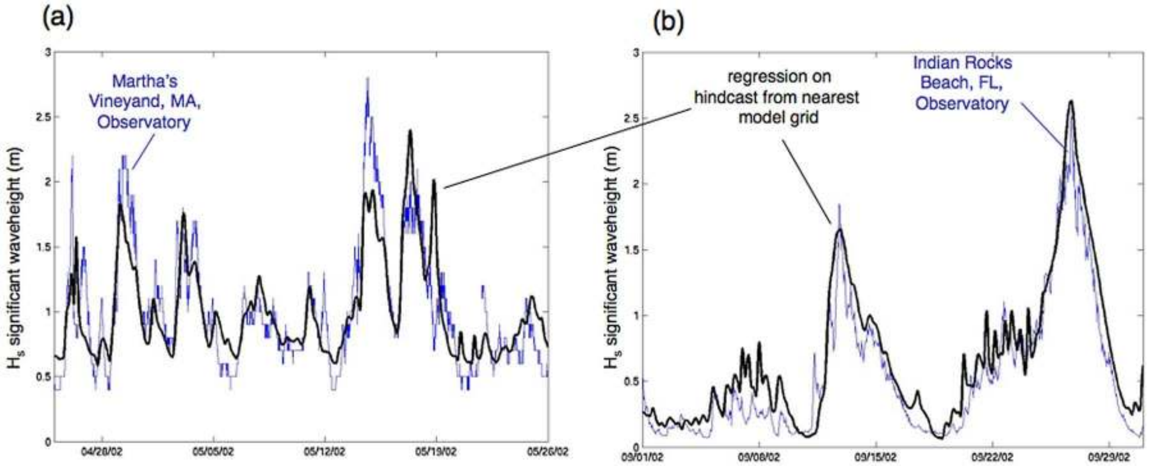

Fig. 4. Portion of historical data used to calibrate WW3 wave predictions for the (a) MVCO and (b) IRB sites. Each case compares observed significant waveheight H_s (thin line) to H_s from the closest WW3 model cell modified by an empirical transform function (thick line).

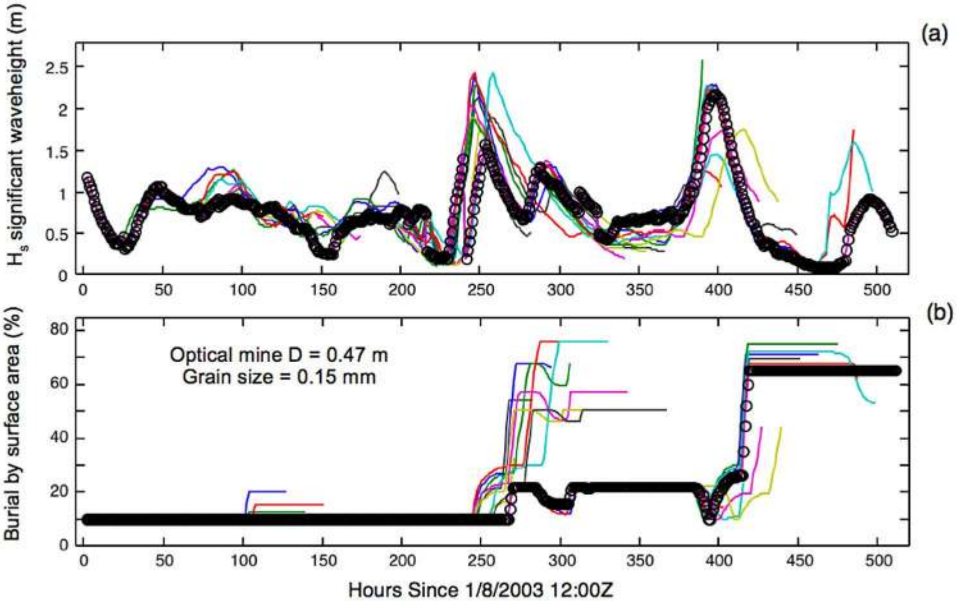

Fig. 5. Sequence of WW3 model wave hindcasts/forecasts for IRB, presented at the Thid Annual ONR MBP Workshop, during IRB field experiment. (a) Significant waveheight and (b) percent burial by surface area. In each case, individual growing five-day forecasts are shown as thin lines. The latest model hindcast/forecast at the time the results were presented is shown as the line of thick black circles. Note the significant variations between individual forecasts and the final hindcast.

modeled burial by surface area with instantaneous infilling. A proxy for percent burial based on the acoustic shadow length estimated from a nearby rotating sidescan sonar is also shown (see [9] for details). For this data set, growing waves initially deepened the scour pit, the mine quickly slid into the scour pit, and sediment episodically infilled the scour pit as waves decayed [7]. To one significant digit, the best comparison between observed and modeled burial by surface area for the calibration case (located in fine sand) occurred for $\alpha = 0.4$ and $f_w = 0.008$. Including instantaneous infilling reproduced the published burial data set quite well. The available data were from an optical mine, which had sensors around its circumference to measure percent burial by surface area, but there was no internal pressure sensor to document burial by depth below the ambient seabed. Based on the available calibration data, infilling was turned on for the subsequent real-time scour forecasting effort for the IRB site.

IV. WAVE MODEL METHODS AND SCOUR FORECAST RESULTS

To forecast mine burial by wave-induced scour, it was necessary to forecast waves for model input. The National Oceanic and Atmospheric Administration (NOAA, Washington, DC) WaveWatch 3 (WW3) wave model chosen for this application is a publicly available, third generation global wave model [22]. The WW3 model provides five-day forecasts of winds and waves with 0.25° resolution in latitude and longitude (see Fig. 2) and a time step of three hours. Model output includes wave parameters such as significant waveheight, wave period, direction of wave propagation, and estimates of East/West (E/W) and North/South (N/S) components of 10-m wind velocity. Occasionally, unrealistic values in predicted wave period generated by the WW3 model complicated attempts to utilize the model wave period output. Therefore, WW3-based predictions utilized a fixed wave period for each site based on

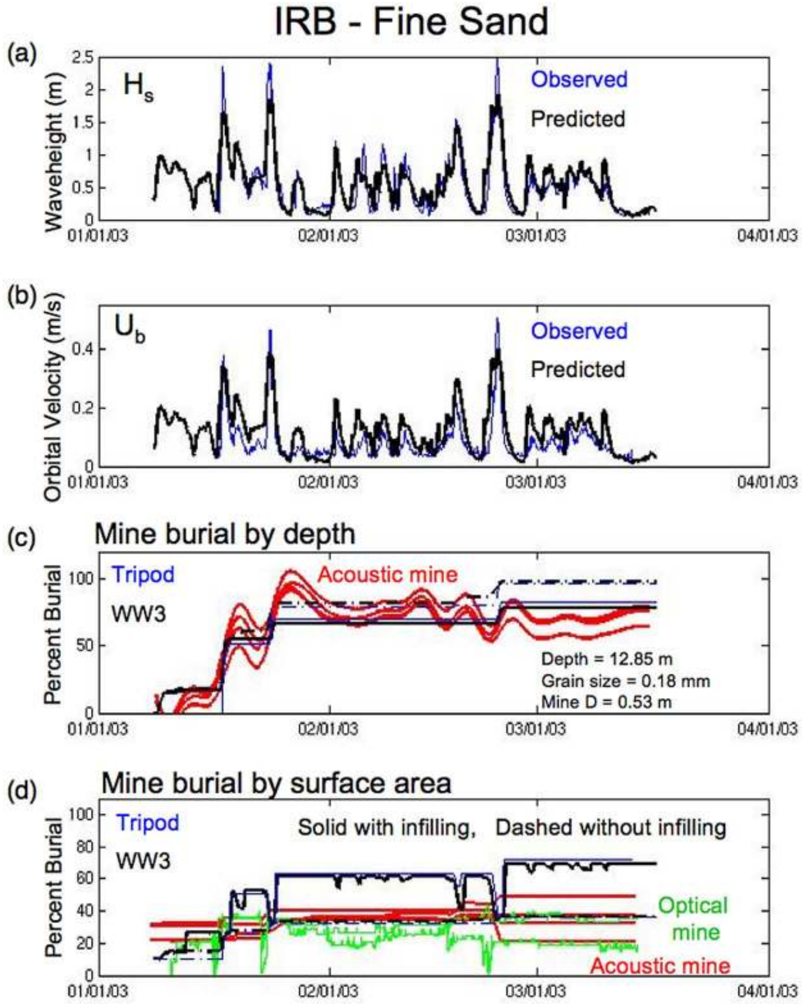

Fig. 6. Summary plots for IRB fine sand deployment. (a) WW3 hindcast H_s regressed to local conditions (thick line) compared to tripod observations (thin line). (b) WW3 hindcast U_b (thick line), based on linear wave theory with $T = 7$ s, compared to observations (thin line). (c) Predicted and observed burial by depth. Thick red lines indicate depth change based on pressure sensors within the acoustic instrumented mines (AIMs) located at the site. (d) Predicted and observed burial by surface area. Thick red lines indicate surface area burial based on acoustic sensors from AIMs, while the thin green lines indicate surface area burial registered by mines with optical sensors. (c) and (d) Scour model results computed either with WW3 hindcast waves (thick black lines) or with tripod measurements (thin blue lines) and with infilling turned on (solid lines) or off (dashed lines). [In grayscale version of panels, in (c) and (d), red and green lines appear gray and blue lines appear black.]

empirical analysis of historical wave records. The characteristic wave period for the MVCO and IRB field sites was set to 6 and 7 s, respectively. WW3 wave and wind forecasts are updated by NOAA twice daily, with the first 12 h of each model run representing hindcast conditions. WW3 output files are available for public download from the NOAA wave model website in the World Meteorological (WMO) gridded binary (GRIB) format [22].

Once extracted, WW3 wave estimates for the nearest model grid point (see Fig. 2) were subsequently converted to local values based on regression analysis of historical time-series measurements of local wave conditions collected in 2002 (Fig. 4). Local estimates of significant waveheight were related to the nearest WW3 grid cell predictions by the following transform functions

$$H_{s(\mathrm{IRB})} = 0.954 H_{s(\mathrm{WW3})} + 0.045 \tag{8}$$

in the case of the IRB site, and

$$H_{s(\mathrm{MVCO})} = 0.194 H^2_{s(\mathrm{WW3})} + 0.084 H_{s(\mathrm{WW3})} + 0.536 \tag{9}$$

in the case of the MVCO site, where the units of waveheight are in meters.

Based on observations, both field sites were described as being wave dominated [7], [18], thus the scour results presented throughout this paper were based on wave forcing alone. Separate model runs were completed that included the combined effects of waves and currents, yet these results indicated negligible difference in comparison to results from the waves-only case [19].

The proof-of-concept scour forecasting exercise focused on the IRB mine burial field experiment, which took place from January to March 2003. Throughout this field experiment, new five-day WW3 wave forecasts were downloaded every 12 h, archived, and wave forecasts for the grid cell nearest the IRB

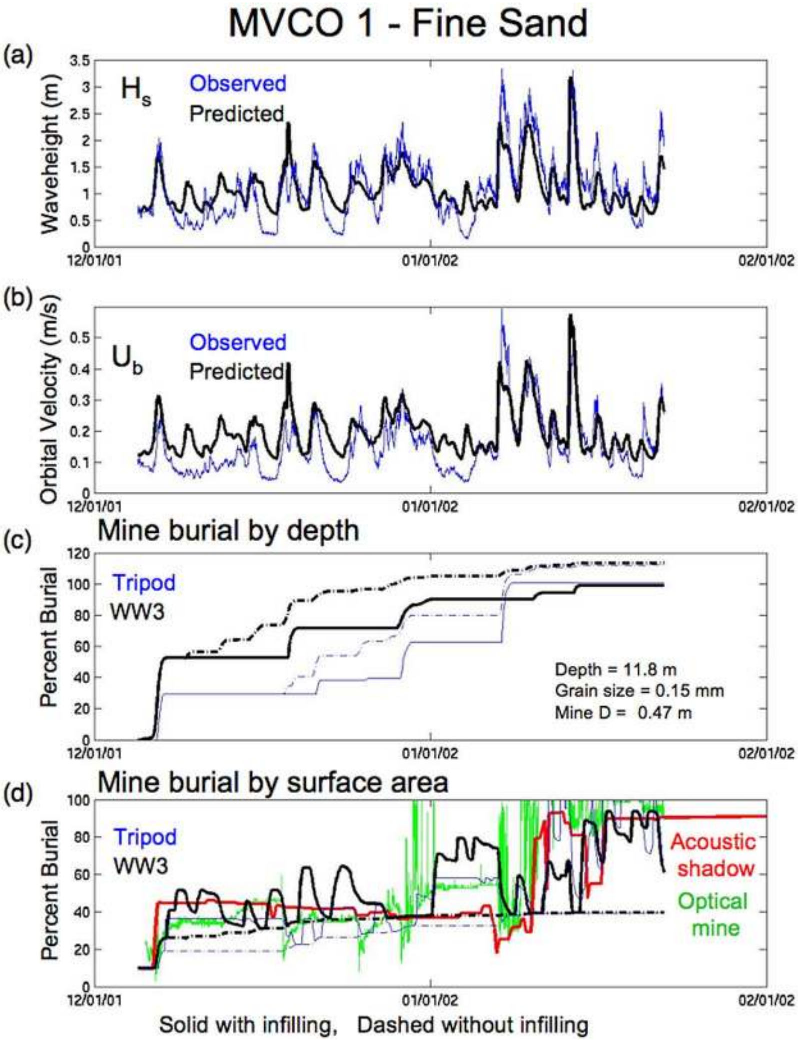

Fig. 7. Summary plots for fine sand, MVCO deployment #1. Figure layout and symbols are the same as in Fig. 6. The thick red line in the fourth panel is burial estimated from acoustic shadow length as in Fig. 3. Note: no directly observed estimates of burial by depth were available for this deployment.

field site were extracted. Linear wave theory (with $T = 7$ s) was then used to forecast the rms amplitude of near-bed rms orbital velocity. [Note that the minor correction provided in (8) was not implemented until our "best-case" hindcasting effort described in Section V.] Next, orbital velocity was entered into (1)–(7) with $a = 0.4$ and $f_w = 0.008$ to forecast mine burial. The first 12 h of any model run represented the hindcast portion of the record. At each time step, the initial portion (12 h) was retained and the subsequent forecast was appended. In this manner, a growing record of model inputs and outputs was created, including a regularly updated five-day forecast of expected mine burial.

Fig. 5 displays real-time mine burial forecasts for the IRB experiment site, as presented at the Third Annual ONR Mine Burial Prediction Workshop, St. Petersburg, FL, January 28–30, 2003, while the instrumented mines were still deployed in the water [23]. Updated forecasts, including five-day forecasts of waveheight, bottom-orbital velocity, and percent mine burial, were released daily on the Internet. To demonstrate the potential for rapid response to changing operational needs, real-time forecasts of mine burial for the northwest Persian Gulf during the early stages of Operation Iraqi Freedom were also developed from publicly available inputs [19].

The results of comparing a series of subsequent forecasts represent a range of possible predicted outcomes (Fig. 5). For example, five-day forecasts for the IRB experiment between hour 250 and 300 initially called for surface burial of up to 75%. As the actual wave event approached, however, the waveheight forecast diminished and the burial forecast eventually dropped to 20%. This situation is similar to comparing the weather recorded on any given day to the weather forecast reported each of the previous mornings. Thus, a main result of this proof-of-concept exercise was the finding that inherent uncertainty in wave forecasting is likely to introduce as much or more error into mine burial forecasts as does uncertainty in the formulation of the mine burial model. Comparison of modeling results to observed burial after the field experiment (see Section V) identified a second major limitation associated with uncertainty in the occurrence of scour pit infilling.

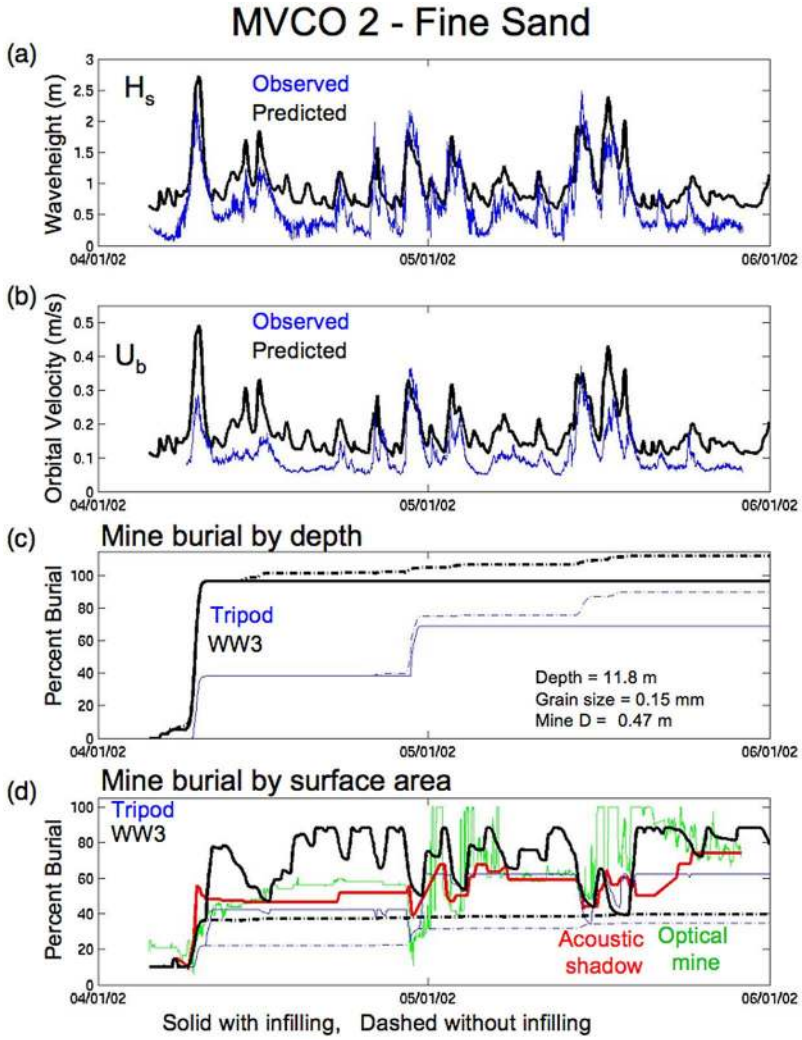

Fig. 8. Summary plots for fine sand, MVCO deployment #2. Figure layout and symbols are the same as in Figs. 6 and 7. Note: No directly observed estimates of burial by depth were available for this deployment.

V. HINDCAST RESULTS FOR SCOUR BURIAL IN FINE SAND

Figs. 6–9 contain hindcasts comparing predicted to observed mine burial for all of the quality-controlled field observations that involved instrumented mine deployments in fine sand ($d = 0.15$ mm at MVCO and $d = 0.18$ mm at IRB). Because of the difference in fine sand grain size between these two sites (and among future sites of interest), burial predictions are not likely to be universally optimized by a single constant f_w. To avoid the arbitrary nature of tuning f_w to each site individually, as well as the possibility that other site-specific model shortcomings might be lumped into a locally best-fit f_w, the constant $f_w = 0.008$ used in the preforecast calibration (Fig. 3) and in the five-day forecasts (Fig. 5) was replaced with a variable f_w based on Swart's [24] formulation, as implemented by Traykovski *et al.* [25]

$$f_w = \exp\left[5.213(d/a_b)^{0.194} - 5.977\right] \qquad (10)$$

where $a_b = U_b T/2\pi$ is the near-bed rms amplitude of the near-bed wave orbital excursion amplitude. The choice of appropriate measure of roughness (d) in (10) is quite variable in the literature, spanning a range anywhere from d to $4d$. Our value for d was based on a $d50$ value, as implemented by Traykovski *et al.* [25].

With f_w determined by (10), the relationship between scour pit depth and partial burial (α) was the only remaining best-fit parameter. In considering all the observed burial data together to one significant digit, a reasonable comparison between observed and modeled burial by surface area occurred for $\alpha = 0.3$. However, α does not play a role in predicting mine burial by depth. Thus, the burial by depth formulation still contained only the recommended coefficients from Whitehouse [11] plus the choice to either include or exclude scour pit infilling.

Once the empirically determined transform functions were applied, WW3 hindcast predictions were seen to estimate the local waveheights reasonably well [Figs. 6(a), 7(a), 8(a), and 9(a)]. The transformed WW3 predictions tended to slightly underpredict significant waveheight during storms and slightly overpredict these values during fair weather. Application of linear wave theory with a constant wave period resulted in a similar trend in fair weather versus storm comparisons for the

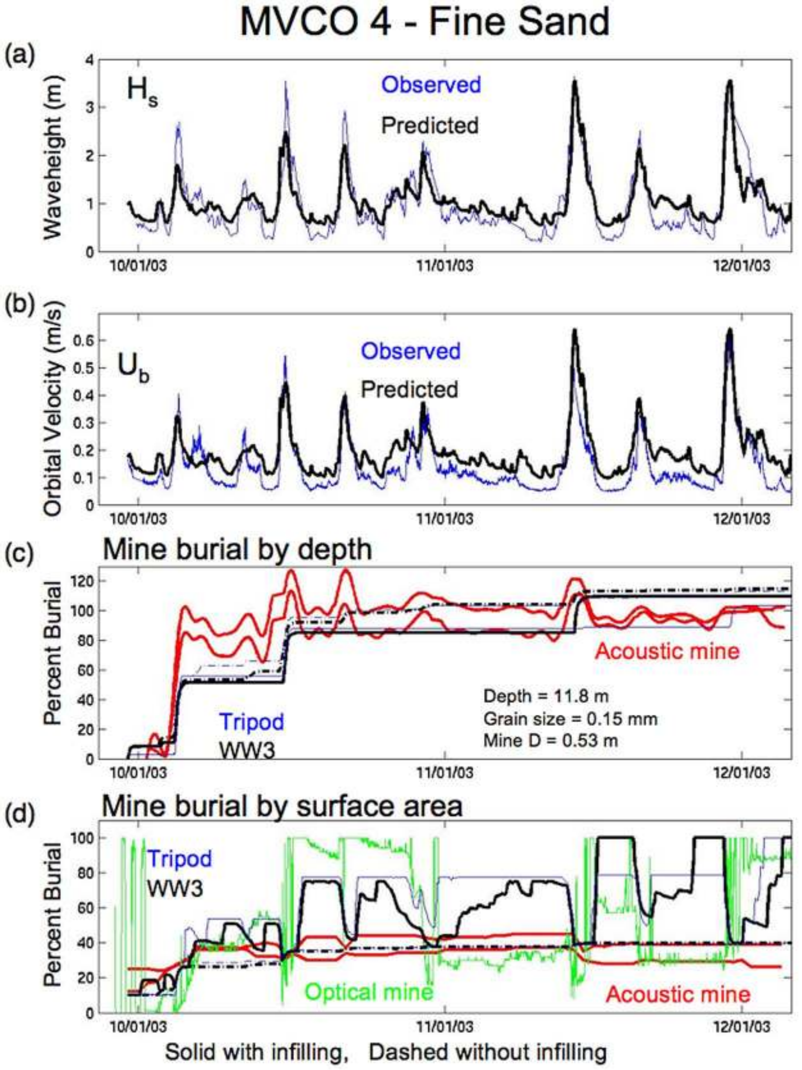

Fig. 9. Summary plots for fine sand, MVCO deployment #4. Figure layout and symbols are the same as in Fig. 6.

rms amplitude of near-bed orbital velocity amplitude [Figs. 6(b)–9(b)]. Errors in estimating low-wave conditions are inconsequential as these waves are incapable of inducing scour. Wave estimates during storm conditions are more critical to accurate forecasts. Wave estimates during high-wave conditions, operatively defined as times with $H_s > 1.5$ m, were generally within 20% of the observed values [19].

Two of the field experiments at fine sand sites (IRB and MVCO #4) included instrumented mines with internal pressure sensors, allowing direct observation of mine burial by depth [Figs. 6(c) and 9(c)]. Effects of short-term variations in sea level and atmospheric pressure were removed as far as possible through comparison to local fixed tide gauges and lowpass filtering [17], [8]. Undulations in the resulting depth records are artifacts of this filtering process. In both of these experiments, the hindcast prediction for mine burial by depth compared reasonably well with observed burial [Figs. 6(c) and 9(c)] with no change in coefficients from those recommended by Whitehouse [11]. The empirical coefficient α is not an issue for burial by depth predictions. Furthermore, burial by depth is relatively insensitive as to whether infilling is included in the model. Burial by depth simply assumes that the mine always slides down to the lowest part of the scour pit that had formed up to that point in time. During the IRB experiment, Wolfson *et al.* [6] independently measured burial by depth in fine sand for one of the acoustic mines using repeated multibeam surveys, and they calculated depths of burial which are highly consistent with the results in Fig. 6(c).

In two of the cases (MVCO 1 and 2), predicted burial by depth using modeled U_b was significantly greater than predicted burial by depth using observed U_b [Figs. 7(c) and 8(c). Even though waveheights during scour events were generally hindcast by WW3 to within about 20% accuracy, the stress, which drives scour, is proportional to U_b^2, further increasing the potential error in scour. Also, if wave period is predicted incorrectly, U_b may be incorrect even when H_s is predicted well. Although hindcast wave predictions are not the largest single source of error, scour predictions are likely to be improved in future applications through use of better resolved local wave models and more sophisticated formulations for U_b that incorporate the entire wave spectrum. While Hrms and Urms appeared to be reliable descriptors for modeling purposes at the two study sites

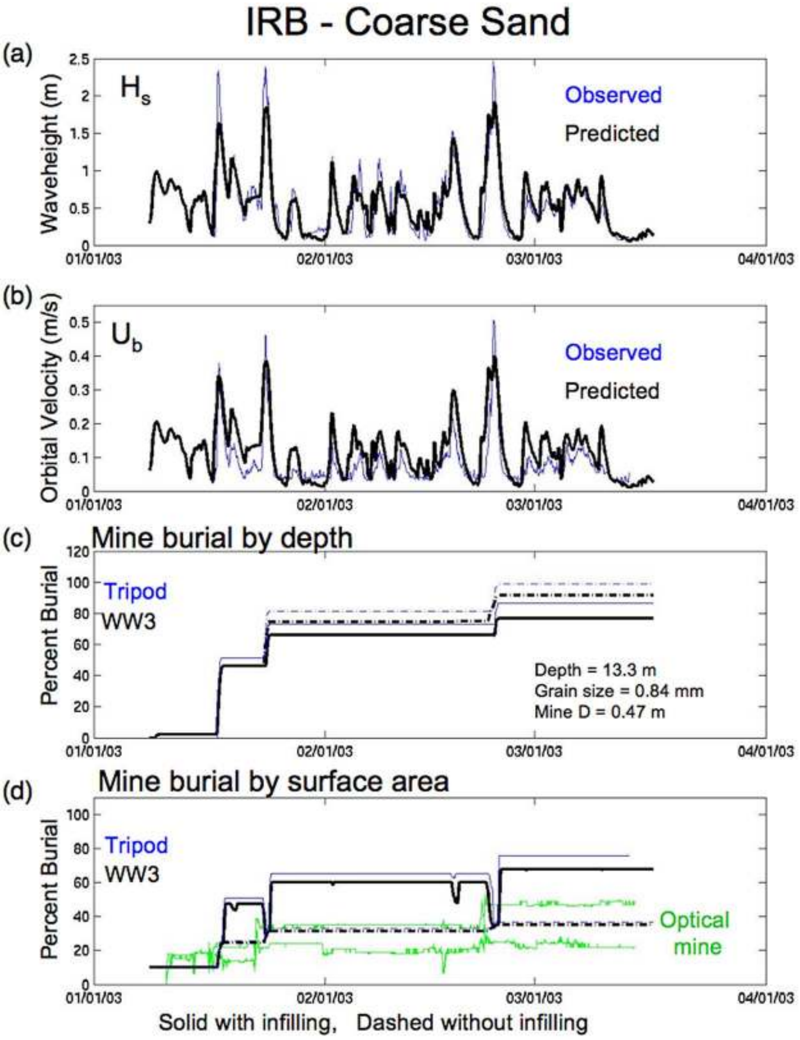

Fig. 10. Summary plots for IRB coarse sand deployment. Figure layout and symbols are the same as in Figs. 6. Note: No direct mine observations of burial by depth were available for this site.

presented here, they might not be good descriptors in all settings where, for instance, the waves might be largely bimodal. Another potential source of error is the assumption that Swart's [24] formulation of f_w provides the best estimate of the true far-field shear stress. However, errors in f_w are unlikely to explain inconsistencies between scour forced by observed versus modeled waves. Therefore, the higher prediction of burial by depth using modeled U_b in Figs. 7(c) and 8(c) suggests the hydrodynamic estimates and not the Whitehouse [11] scour equations are the main source of the discrepancies.

In contrast to burial by depth, predicted burial by surface area is highly sensitive to infilling. Observed burial by surface area for the IRB fine sand deployment was better predicted with infilling turned off Fig. 6(d). Conversely, observed burial by surface area for the first two Martha's Vineyard deployments [Figs. 7(d) and 8(d)] was clearly better predicted with infilling turned on. Infilling during wave decay is more likely off Martha's Vineyard because of the presence of highly mobile fine sediment at the site that periodically settles into the scour pits [7], [9]. Such high concentrations of fine material are not present off IRB. However, infilling does not always occur off MVCO [see acoustic mine data in Fig. 9(d)], and at present there is no conclusive theory for predicting where and when infilling will or will not occur.

Even within time-series from individual deployments, as illustrated by the optical mines during the MVCO deployment # 1 and #4 [Figs. 7(d) and 9(d)], there are alternating periods in the record that exhibit no infilling followed by complete infilling. Nonetheless, the two extreme predictions of surface area burial provide a useful envelope of likely outcomes. It is interesting to note that during MVCO deployment #4, the optical mine detected frequent oscillations between complete infilling and complete scour, while the acoustic mine consistently showed no infilling. The rapid changes in infilling and lack of detection by acoustics suggests a very easily disturbed, acoustically transparent muddy pool might have been advected in and out of the scour pit.

VI. HINDCAST RESULTS FOR SCOUR BURIAL IN COARSE SAND: BEDFORM-LIMITED SCOUR

Figs. 10–12 compare model hindcast estimates and observed data for mine deployments within coarse sands. In each case,

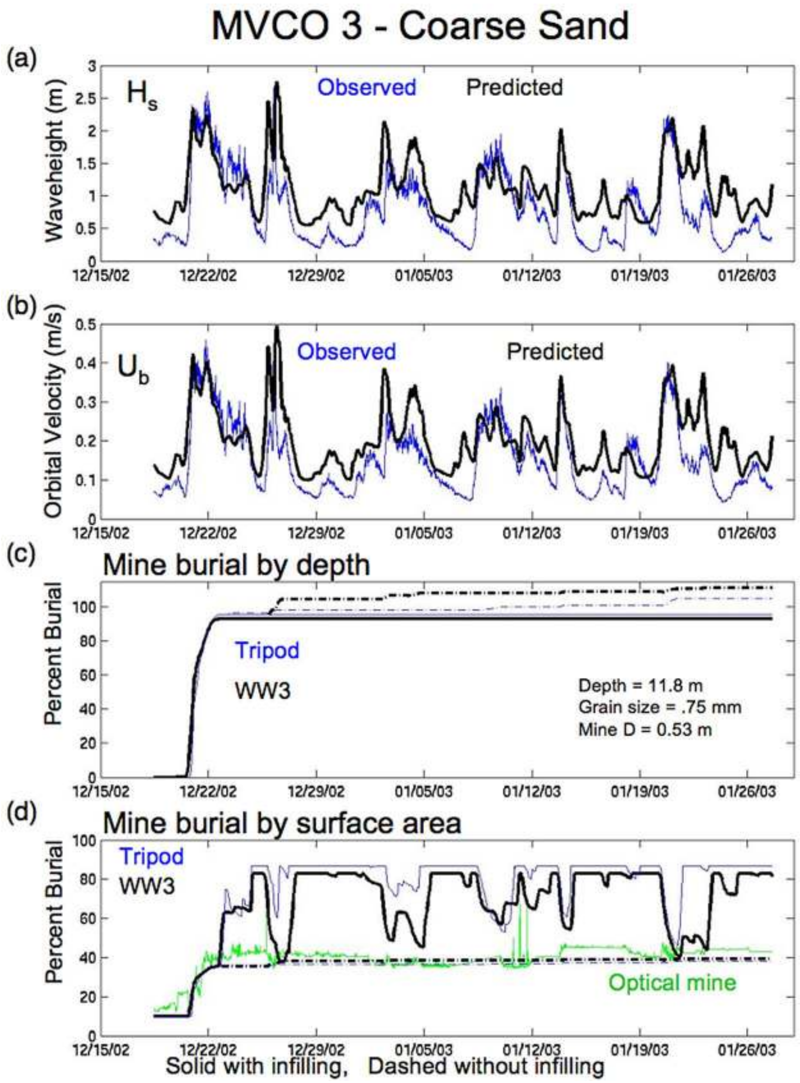

Fig. 11. Summary plots for coarse sand, MVCO deployment #3. Figure layout and symbols are the same as in Fig. 6. Note: no directly observed estimates of burial by depth were available for this deployment.

data existed to compare model estimates of burial by surface area [Figs. 10(d)–12(d)], with one case in which time-series data also existed to compare estimates of burial by depth [Fig. 12(c)]. For the first two cases [Figs. 10(d) and 11(d)], the model does a better job of predicting burial by surface area when infilling is turned off. In this respect, the results for burial by surface area on coarse sand for MVCO deployment #3 [Fig. 11(d)] are opposite to those on fine sand for MVCO deployments #1 and #2 [Figs. 7(d) and 8(d)], where burial by surface area was better predicted with infilling turned on. The turbulence induced by much larger wave orbital ripples within the coarse sand domain [26] may make it more difficult for any available fine sediment to settle into the scour pit. The nature of the scour pits themselves is quite distinct in the coarse sand settings. According to sonar observations by Traykovski *et al.* [9] the scour pits in the coarse sand at MVCO are much smaller both in lateral extent and depth than those found in fine sand.

In the one deployment case for which time-series data for burial by depth data were available [Fig. 12(c)], the model is seen to do a fairly poor job of predicting the long-term depth behavior of the mines. The model does a good job with the initial predictions up to and including the first wave event, but the mines fail to respond to subsequent wave events with any appreciable scour. Details of the hydrodynamics (wave and current velocities) and sediment transport dynamics (e.g., Shields parameter) can be found in [9]. A similar pattern was reported by Wolfson *et al.* [6] for one of the optical mines on coarse sand at IRB based on multibeam bathymetry surveys. Wolfson *et al.* [6] found that burial by depth at the coarse IRB site was initially consistent with model predictions, but predictions significantly overestimated the observed burial over the remainder of the experiment.

The shallow burial by depth in coarse sand followed by a lack of further response is in stark contrast to that seen during the fine sand deployments. In fine sand, the mines were observed to continue to respond to storm events until the mine was flush with the ambient seabed. Instead, the mines in coarse sand appear to scour to a shallow depth during the first major wave event such that they stick up slightly above the surrounding field of large wave orbital ripples, as illustrated in Fig. 13. Estimates from a rotary sonar system deployed nearby indicated that the tops of the mines were approximately 30% higher than the ambient

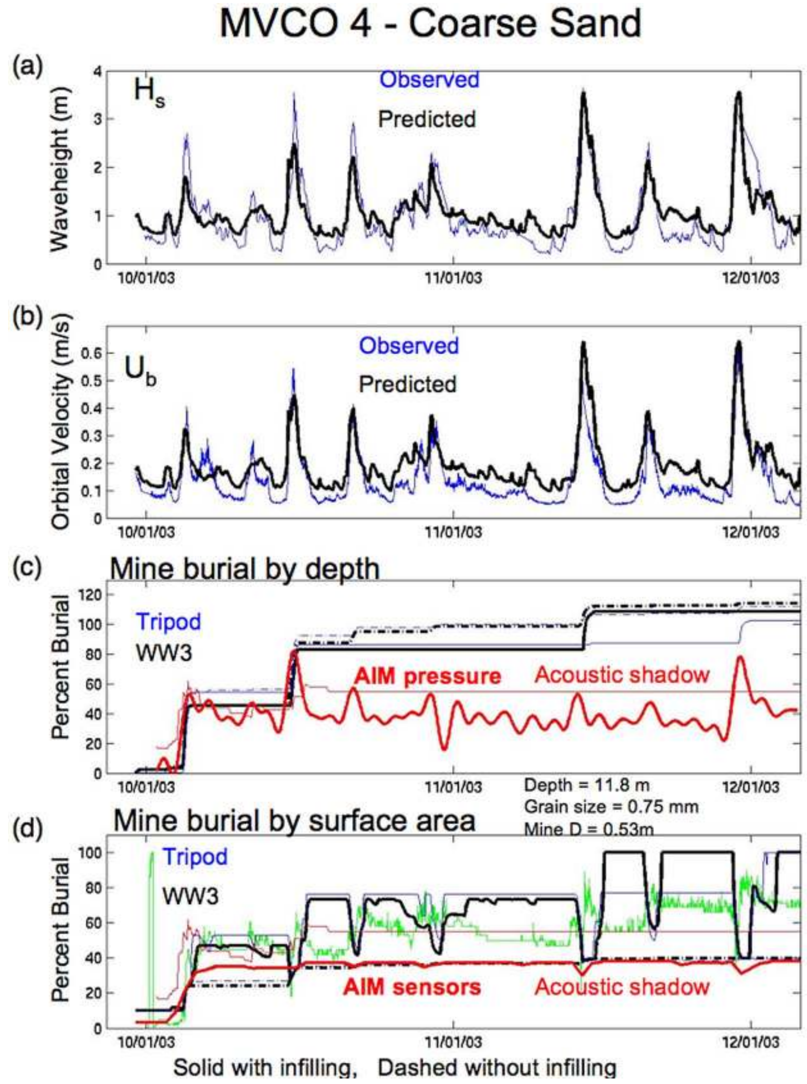

Fig. 12. Summary plots for coarse sand, MVCO deployment #4. Figure layout and symbols are the same as in Figs. 6 and 7 except that thin red lines are depths inferred from acoustic shadows and thick red lines are inferred from AIMs.

active ripples [9]. This finding suggests that the bedforms themselves may be acting to limit the depth of scour once the mine presents itself to the flow with a roughness approximately equal to the bedforms. At that stage, the mine no longer perturbs the flow beyond the ambient bedforms, and the scour mechanism based on locally enhanced vortex shedding shuts down.

A fairly straightforward empirical way to address the effect of bedform-limited scour is to use a bedform model to predict the ripple dimensions and use the sonar coefficient estimate to set a maximum scour depth. In Fig. 14, the model estimates of burial by depth (C) and burial by surface area (D) were computed based on a depth-limited scour set by the bedform dimensions calculated from the Wiberg and Harris [27] equations. In their laboratory experiments using small cylinders, Voropayev *et al.* [15] noted distinct burial behavior in the presence and absence of large ripples. They found that if the diameter of the cylinder was less than the ripple height, ripple effects became dominant over cylinder-induced scour, and ripples propagated past the cylinder without the formation of sustainable scour pits. They termed this state "periodic burial."

The bedform correction developed here can be employed in all settings to avoid any arbitrary usage. However, the correction only significantly contributes to the result in coarse sediments that support large wave orbital ripples. In fine sand settings with small anorbital-scale ripples, the small heights of the ripples (O 1 cm) leads to a trivial correction to the scour depth.

VII. THE 2-D WEB-BASED INTERACTIVE MODEL

To investigate spatial variability and model sensitivity over scales of tens to hundreds of meters and simultaneously provide model results to end users in an easily conveyed and utilized format, a web-based mine burial model with a 2-D graphical user interface (GUI) was developed and maintained from the Virginia Institute of Marine Science (VIMS) MBP website. Web-browser plug-in support is freely available for both PC and Macintosh platforms. Examples of the interactive instrument panel are shown in Fig. 15(a) (IRB) and Fig. 15(b) (Martha's Vineyard). This remotely operable 2-D model was used by Wolfson *et al.* [6] to compare predicted scour-induced

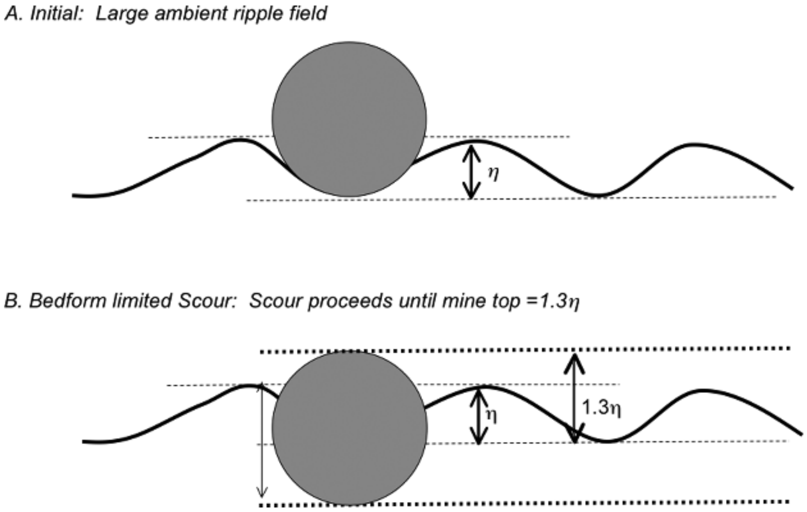

Fig. 13. Diagram of bedform-limited scour in the presence of large wave orbital ripples. (a) Initial vertical position of mine within ripple field. Note: The top of the mine stands well above the ambient ripples. (b) Vertical position of mine after energetic storm event. Note: the top of the mine now stands a smaller fraction above the ambient ripples.

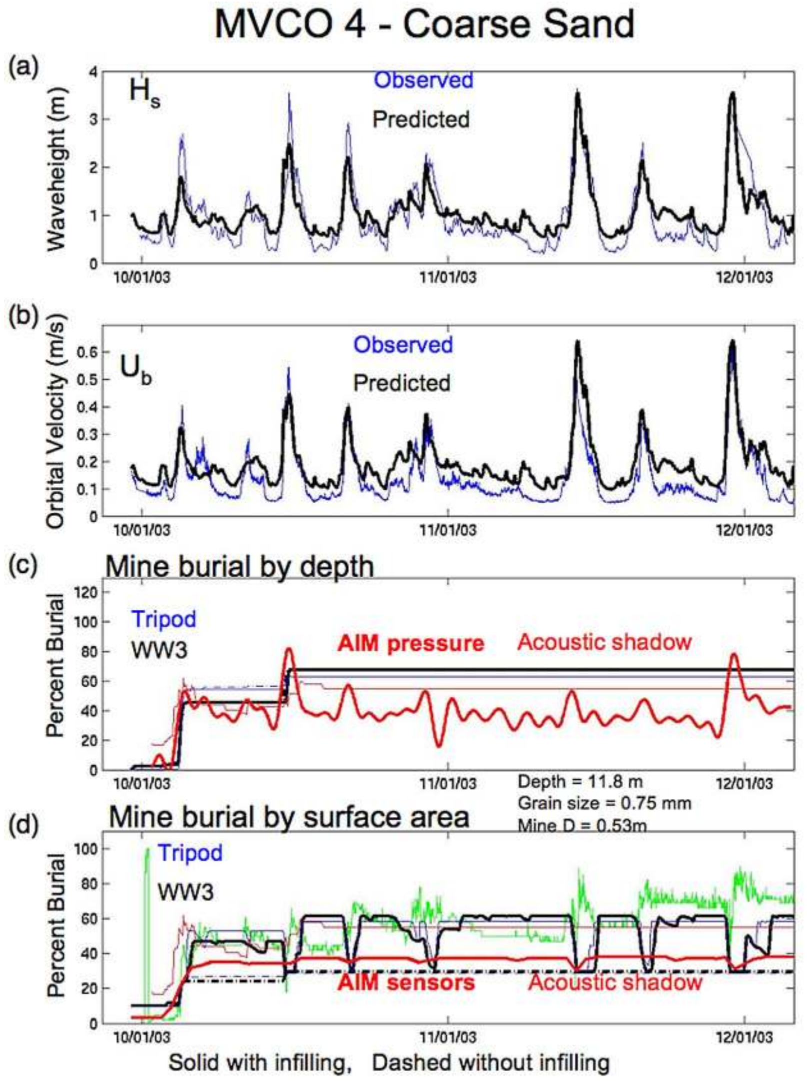

Fig. 14. Summary plots for coarse sand, MVCO #4, including additional parameterizations for bedform-limited scour. Figure layout and symbols are the same as in Fig. 13.

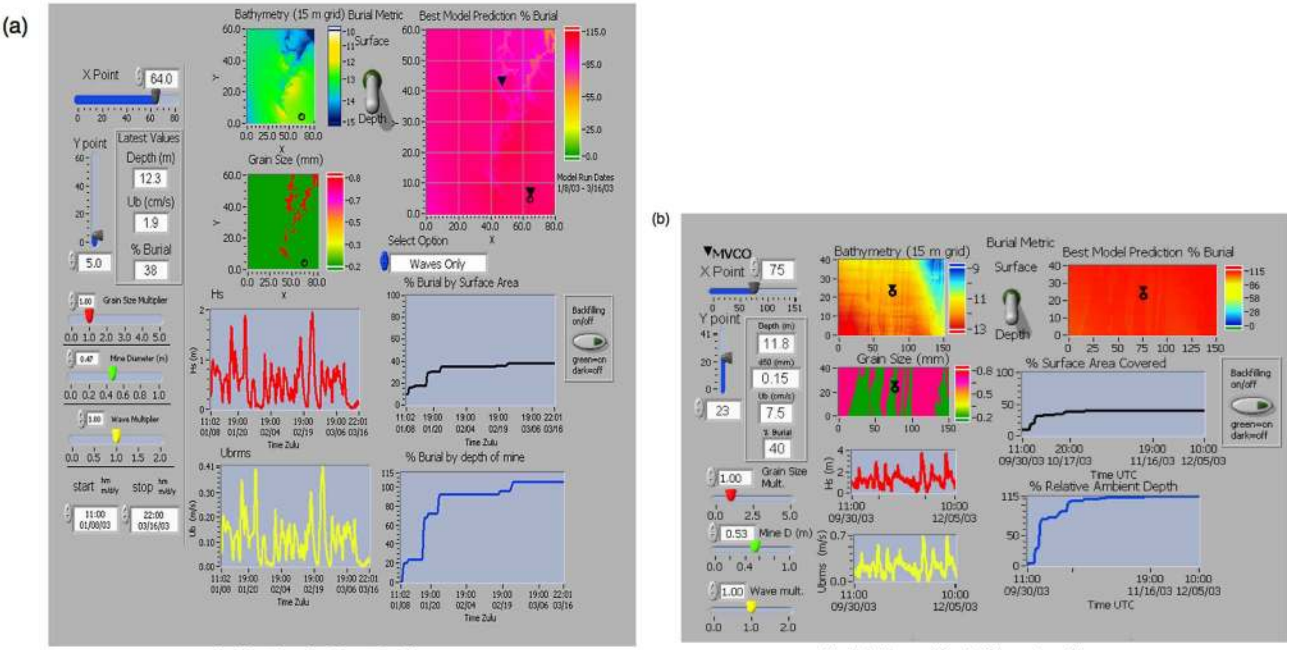

X Point 64.0
Y point 5.0
Depth (m) 12.3
Ub (cm/s) 1.9
% Burial 38
Grain Size Multiplier 1.00
Mine Diameter (m) 0.47
Wave Multiplier 1.00
start 11:00 01/08/03
stop 22:00 03/16/03
Select Option Waves Only

X Point 75
Y point 23
Depth (m) 11.8
d50 (mm) 0.15
Ub (cm/s) 7.5
% Burial 40
Grain Size Mult. 1.00
Mine D (m) 0.53
Wave mult. 1.00

Indian Rocks Beach, FL

Martha's Vineyard Coastal Observatory, MA

Fig. 15. Web-based GUI models for (a) IRB and (b) MVCO field sites. These interactive models were available online during the ONR MBP program.

mine burial with that observed at IRB using repeated multibeam observations.

The GUI allows users to both evaluate specific case scenarios of mine diameter, grain size, and wave conditions as well as offers the ability to explore the sensitivity of model predictions to variations in input parameters (e.g., adjusting waveheight by a factor of $+/-2$). Users can turn the effect of scour pit infilling on or off and immediately observe the changes produced in the estimates of burial by depth and burial by surface area. The user can also select and interrogate any grid point in the model domain. The 2-D local bathymetry and grain-size variability are referenced from the included plan-view plots. In addition, the plan-view map of final mine condition can be referenced either in terms of burial by depth or burial by surface area. Users also have control over the start and stop time of the simulation, which can be used to evaluate the hysteresis effect of events on scour. The interactive models were based on gridded bathymetry with hourly time steps in hydrodynamic forcing.

The 2-D inputs and outputs of the GUI highlight the small-scale spatial variations in scour-induced burial that result from variations in bathymetry and grain size. Like many sandy inner shelf systems around the world [26], [28], the two field sites examined in this paper are typified by complex heterogeneity at a range of spatial scales [18], [20]. Sharp changes in grain size, composition, and bedform roughness produce significant variations in model estimates of burial. The present form of the 2-D interactive model does not include bedform-limited scour, an effect that markedly enhances grain-size-dependent differences in scour burial. The resulting variations in scour-induced burial can occur over relatively short distances (O 10 m) often below the resolution of most geologic maps but large enough to be of concern for mine countermeasure operations. The implication for mine burial is that adjacent corridors of very different scour response are likely to be seen in close proximity on the inner shelf, despite similar wave forcing and generally sandy conditions.

Clear examples of the spatial variability in grain size common to natural settings are illustrated in Fig. 15(a) and (b). Subplots show in plan view patterns of contrasting fine (green) and coarse sand (pink to red). The patches of coarse material coincide with slight depressions in the seafloor of between 30–50 cm and are termed sorted bedforms or rippled scour depressions [20], [26]. Such small-scale variations in grain size remain one of the greatest sources of uncertainty in mine burial prediction efforts and are often not reconciled in available geologic maps.

VIII. DISCUSSION AND CONCLUSION

In this paper, a simple parameterized model for wave-induced burial of cylindrical mine-like objects was developed, building on well-established engineering equations for the depth of scour pits around seabed objects. The resulting model is a function of grain-size, time-varying, near-bed wave orbital velocity and mine diameter. Calculation of burial by depth assumed the mine settles into its scour pit such that the depth of the mine below the ambient seabed is equal to the greatest depth the scour pit has reached up to that point in time. The following two extremes for scour pit infilling were considered: 1) instantaneous infilling back to a pit depth in equilibrium with far-field bed stress (infilling turned "on") and 2) occurrence of a relict scour pit with no additional infilling during wave decay (infilling turned "off"). Burial by surface area was then calculated by assuming the object was covered by sediment up to a fixed level proportional to the overall depth of the scour pit. Predicted burial by depth is independent of this empirical fraction and is insensitive to whether infilling is turned on or off.

Comparison of model predictions to the observed burial of instrumented inert mines deployed at sandy inner shelf sites off the MVCO and off IRB showed that the scour model parameters provided by Whitehouse [11] for self-settling horizontal cylinders worked well for scour around O (0.5 m) diameter cylindrical mines in fine sand. Observed and predicted burial by depth agreed well despite the fact that the Whitehouse parameters were developed for short cylinders in fine sand, exposed to steady flow conditions. Previous observations have suggested that steady flow scour relations should overestimate scour observed under oscillatory flow conditions.

Prediction of percent burial by surface area was more ambiguous, mainly because no definitive theory exists for predicting whether infilling will occur. Nonetheless, infilling turned on or off provided a finite envelope of predicted burial by surface area that was consistent with observations. Rapid scour pit infilling was often seen at MVCO but never at IRB, suggesting that the environmental presence of fine sediment plays a key role in promoting infilling. At MVCO, infilling was observed less frequently over coarse than over fine sand, and was imaged less clearly by acoustic than by optical mines. These observations imply that easily suspended, sometimes acoustically transparent mud can move rapidly in and out of the scour pits, and the turbulence generated by large wave orbital ripples on the coarse sand may inhibit its deposition.

The feasibility of predicting mine burial using a widely available wave model was tested in both forecast and hindcast mode. In hindcast mode, the NOAA WW3 model was found to predict waveheight well, particularly when modified using a simple local regression based on historical waveheights. Prediction of wave period by WW3 was more erratic, and locally constant wave periods were implemented to facilitate prediction of bottom orbital velocity. Based on linear wave theory, WW3 hindcasts of bottom orbital velocity were then usually found to be within $+/-20\%$ of observed values during energetic events. For the cases with scour observations available from instrumented mines, the differences between burial predictions based on observed versus hindcast orbital velocities were smaller than the typical disagreement between observed and predicted burial. Thus, hindcast waves provided by readily available wave models are adequate for useful operational forcing of mine burial predictions.

During the IRB mine burial field experiment, five-day forecasts of regional waveheights updated every 12 h were used to generate real-time forecasts of local waveheight and near-bed wave orbital velocities that were posted to the web. These wave forecasts were, in turn, used to forecast mine burial, and mine burial forecasts were likewise posted and presented to MBP investigators in real time during the experiment. Due to inherent uncertainty associated with weather forecasting, evolving five-day wave forecasts introduced larger errors into subsequent burial depth estimates than those errors associated with the formulas for mine burial in fine sand.

Although predictions of percent burial by surface area were equally accurate for mines placed in coarse or fine sand, predictions of burial by depth in coarse sand based on the Whitehouse coefficients [11] significantly overestimated the observed depth of burial. A logical explanation is that mines in a ripple field bury via the effect of locally enhanced vortex shedding only while the portion of the mine protruding above the ambient seabed produces more intense turbulence than the ambient turbulence produced by the surrounding ripples. Within a field of coarse sand containing large orbital ripples, this state is likely to be reached at a modest degree of burial. In this paper, a simple approach was implemented such that an established bedform model was used to predict ripple dimensions, and observations of burial were then used to empirically derive an equilibrium mine protrusion height.

Several key factors that account for model uncertainty deserve mentioning here in summary in descending order of importance. First, efforts to forecast wave conditions are one of the largest sources of uncertainty in attempts to predict mine burial days to weeks in advance. Wave forecast error is large far in advance, but much smaller in hindcast mode. Second, spatial heterogeneity of grain size and bedform roughness is a large and often poorly constrained source of uncertainty that can introduce model error both in hindcast and forecast scenarios. Third, the existence of an available pool of mobile fine sediment for scour pit infilling is not well understood and affects burial by surface area greatly, though with minimal effect on burial by depth estimates. It is important to have knowledge on the availability of fine sediment near the burial area and the potential for its transport to the burial area during energetic events. Finally, the relationship between scour pit depth and surface area burial is still poorly constrained and affects both forecast and hindcast estimates.

Future research into mine burial within heterogeneous wave-dominated sandy shelf settings should include attempts to more realistically parameterize bedform behavior. This paper implemented Whitehouse [11] parameterizations for scour by steady flow, but a future study should use the MBP field observations (e.g., grain size, wave period, mine size, and shape, etc.) to derive optimized parameter values and to better test the effect of finite wave period at field scales via inclusion of the Keulegan–Carpenter number. Further laboratory and field analysis is also required to determine the appropriate empirical values for use with more complex mine shapes. A critical issue for modeling surface area burial will be to determine the precise conditions that trigger scour pit infilling. Even in the absence of infilling, it will be important to know how long scour pits will remain relict. Finally, to integrate this scour model into larger probabilistic operational systems, it will be necessary to better describe the statistical distribution of scour prediction outcomes and associated errors.

ACKNOWLEDGMENT

The authors would like to thank R. H. Wilkens, T. Drake, and B. Almquist for the support and program guidance. They would also like to thank the staff at the NRL, the University of South Florida (USF, Tampa, FL), and WHOI for their efforts throughout the field experiments. The WaveWatch3 model was developed and maintained by NOAA's National Center of Environmental Prediction (NCEP).

REFERENCES

[1] R. H. Bennett and R. Dolan, "Mine burial assessment state-of-the-art science, technology, and modeling: A review of coastal research, modeling, and Naval operational needs in shallow water environments with recommendations," Seaprobe, Inc., Tech. Rep. 51-099-05, 2001, p. 106.

[2] D. L. Inman and S. A. Jenkins, Scripps Inst. Oceanogr., "Scour and burial of bottom mines: A primer for fleet use," SIO Ref. Ser. No. 02-8, 2002, p. 127.

[3] R. Wilkens and M. D. Richardson, "Mine burial prediction: A short history and introduction," *IEEE J. Ocean. Eng.*, vol. 32, no. 1, pp. 3–9, Jan. 2007.

[4] G. R. Bower *et al.*, "Indian Rocks Beach experiment January–March 2003," Naval Res. Lab., Stennis Space Center, MS, NRL Memorandum Rep., 2004, p. 101.

[5] M. D. Richardson *et al.*, "Mine burial by scour: preliminary results from the gulf of Mexico," in *Proc. Oceans: Mar. Technol. Ocean Sci. Conf.*, 2004, pp. 2349–2350.

[6] M. L. Wolfson, D. S. Naar, P. A. Howd, S. D. Locker, B. T. Donahue, C. T. Friedrichs, A. C. Trembanis, M. D. Richardson, and T. F. Wever, "Multibeam observations of mine burial near Clearwater, FL, including comparisons to predictions of wave-induced burial," *IEEE J. Ocean. Eng.*, vol. 32, no. 1, pp. 103–118, Jan. 2007.

[7] M. D. Richardson and P. Traykovski, "Real-time observations of mine burial at the Martha's Vineyard Coastal Observatory," in *Proc. 5th Int. Symp. Technol. Mine Problem*, 2002.

[8] J. Bradley, S. Griffin, M. Thiele, Jr., M. D. Richardson, and P. D. Thorne, "An acoustic-instrumented mine for studying subsequent burial," *IEEE J. Ocean. Eng.*, vol. 32, no. 1, pp. 64–77, Jan. 2007.

[9] P. Traykovski, M. D. Richardson, L. A. Mayer, and J. D. Irish, "Mine burial experiments at the Martha's Vineyard Coastal Observatory," *IEEE J. Ocean. Eng.*, vol. 32, no. 1, pp. 150–166, Jan. 2007.

[10] R. Soulsby*, Dynamics of Marine Sands: A Manual for Practical Applications*. London, U.K.: Thomas Telford, 1997.

[11] R. Whitehouse*, Scour at Marine Structures, A Manual for Practical Applications*. London, UK: Thomas Telford, 1998.

[12] B. M. Sumer and J. Fredsøe*, The Mechanics of Scour in the Marine Environment*. Singapore: World Scientific, 2002.

[13] A. C. Trembanis and J. E. McNinch, "Predicting scour and maximum settling depths of shipwrecks: a numeric simulation of the fate of Queen Anne's revenge," in *Proc. Int. Conf. Coastal Sediments*, Clearwater Beach, FL, 2003, CD-ROM.

[14] B. M. Sumer, N. Christiansen, and J. Fredsøe, "Time scale of scour around a vertical pile," in *Proc. 2nd Int. Offshore Polar Eng. Conf.*, San Francisco, CA, 1992, vol. 3, pp. 308–315.

[15] S. I. Voropayev, F. Y. Testik, H. J. Fernando, and D. L. Boyer, "Burial and scour around short cylinder under progressive shoaling waves," *Ocean Eng.*, vol. 30, pp. 1647–1667, 2003.

[16] B. M. Sumer, C. Truelsen, T. Sichman, and J. Fredsøe, "Onset of scour below pipelines and self-burial," *Coastal Eng.*, vol. 24, no. 4, pp. 313–335, 2001.

[17] G. R. Bower, M. D. Richardson, K. B. Briggs, P. A. Elmore, E. F. Braithwaite III, J. Bradley, S. Griffin, T. F. Wever, and R. Lühder, "Measured and predicted burial of cylinders during the Indian Rocks Beach experiment," *IEEE J. Ocean. Eng.*, vol. 32, no. 1, pp. 91–102, Jan. 2007.

[18] P. Howd and J. Brodersen, "Climatology of the bottom boundary layer and an acoustic proxy for sediment suspension on the West Florida inner shelf," presented at the ONR Mine Burial Prediction 3rd Annu. Meeting, St. Petersburg, FL, Jan. 28–29, 2003.

[19] A. C. Trembanis, "Complex inner shelf environments: Observations and modeling of morphodynamics and scour processes," Ph.D. dissertation, Dept. Phys. Sci., VIMS, College of William and Mary, Gloucester Point, FL, 2004.

[20] J. A. Goff, L. A. Mayer, P. Traykovski, I. Buynevich, R. H. Wilkens, R. Raymond, G. Glang, R. L. Evans, H. Olson, and C. Jenkins, "Detailed investigation of sorted bedforms, or "rippled scour depressions," within the Martha's Vineyard Coastal Observatory, Massachusetts," *Continental Shelf Res.*, vol. 25, pp. 461–484, 2005.

[21] S. A. Jenkins, D. L. Inman, M. D. Richardson, T. F. Wever, and J. Wasyl, "Scour and burial mechanics of objects in the nearshore," *IEEE J. Ocean. Eng.*, vol. 32, no. 1, pp. 78–90, Jan. 2007.

[22] H. Tolman, "User manual and system documentation of WAVEWATCH-III version 2.22," NOAA/NWS/NCEP/MMAB Tech. Note 222, 2002, p. 133.

[23] C. T. Friedrichs and A. C. Trembanis, "Forecasting scour related mine burial using a parameterized model," presented at the 3rd Annu. ONR Mine Burial Prediction Workshop, St. Petersburg, FL, Jan. 28–30, 2003.

[24] D. Swart*, Offshore Sediment Transport and Equilibrium Beach Profiles*. Delft, The Netherlands: Delft Hydraulics Lab., 1974, Publication no. 131.

[25] P. Traykovski, A. E. Hay, J. D. Irish, and J. F. Lynch, "Geometry, migration, and evolution of wave orbital ripples at LEO-15," *J. Geophys. Res.*, vol. 104, no. C1, pp. 1505–1524, 1999.

[26] A. C. Trembanis, L. D. Wright, C. T. Friedrichs, M. O. Green, and T. M. Hume, "The effects of spatially complex inner shelf roughness on boundary layer turbulence and current and wave friction: Tairua Embayment, New Zealand," *Continental Shelf Res.*, vol. 24, pp. 1549–1571, 2004.

[27] P. Wiberg and C. Harris, "Ripple geometry in wave-dominated environments," *J. Geophys. Res.*, vol. 99, no. C1, pp. 775–789, 1994.

[28] K. T. Holland, T. R. Keen, J. M. Kaihatu, and J. Calantoni, "Understanding coastal dynamics in heterogeneous sedimentary environments," in *Proc. Int. Conf. Coastal Sediments*, Clearwater Beach, FL, 2003, CD-ROM.

Arthur C. Trembanis received the B.S. degree in geology and oceanography from Duke University, Durham, NC, in 1998 and the Ph.D. degree in marine science from the College of William and Mary, Virginia Institute of Marine Science, Gloucester Point, FL, in 2004.

He completed a Fulbright Fellowship at Sydney University, Sydney, Australia, in 1999. He worked as a Lead Software Developer and Staff Geophysicist in the autonomous underwater vehicle (AUV) industry with Sias Patterson Inc., Yorktown, VA, before conducting a joint WHOI-USGS postdoctoral fellowship at the Woods Hole Oceanographic Institution. Currently, he is an Assistant Professor in the Department of Geology, the University of Delaware, Newark, and Founding Director of the Coastal Sediments, Hydrodynamics, and Engineering Laboratory (CSHEL) there. He has extensive experience in conducting and analyzing complex field studies from sites around the world. His research interests are in the measuring and modeling of coastal morphodynamics particularly beach erosion, beach nourishment, bedform behavior, and scour processes associated with seafloor objects including shipwrecks and mines.

Carl T. Friedrichs received the B.A. degree in geology from Amherst College, Amherst, MA, in 1986 and the Ph.D. degree in oceanography from the Massachusetts Institute of Technology/Woods Hole Oceanographic Institute Joint Program, Woods Hole, MA, in 1993.

He has been on the faculty of the Virginia Institute of Marine Science/School of Marine Science, College of William and Mary, Gloucester Point, FL, since 1993. His research interests are in the areas of estuarine and coastal oceanography, bottom boundary layer physics, sediment transport, and sedimentation.

Michael D. Richardson received the B.S. degree in oceanography from the University of Washington, Seattle, in 1967, the M.S. degree in marine science from the College of Williams and Mary, Williamsburg, VA, in 1971, and the Ph.D. degree in oceanography from the Oregon State University, Corvallis, in 1976.

He began working at the U.S. Naval Ocean Research and Development Activity, now part of the Naval Research Laboratory (NRL), Stennis Space Center, MS, in 1977. Except for a five-year assignment as a Principle Scientist at NATO's SACLANTCEN, La Spezia, Italy (1985–1989), he has worked at NRL as a Research Scientist and is currently the Head of the Seafloor Sciences Branch in the Marine Geosciences Division. His research interests include the effects of biological and physical processes on sediment structure, behavior, and physical properties near the sediment-water interface. His current research is linked to high-frequency acoustic scattering from and propagation within the seafloor and prediction of mine burial.

Dr. Richardson is a Fellow in the Acoustical Society of America, and a member of the American Geophysical Union (AGU), the European Geophysical Society, and Sigma Xi.

Peter Traykovski received the B.S.E. degree in mechanical engineering from Duke University, Durham, NC, in 1988 and the M.S./Engineers degree and Ph.D. degree in applied ocean sciences and engineering from the Massachusetts Institute of Technology/Woods Hole Oceanographic Institution Joint Program, Woods Hole, MA, in 1994 and 1998, respectively.

Currently, he is an Associate Scientist at the Applied Ocean Physics and Engineering Department, the Woods Hole Oceanographic Institution. His main research interests are sediment transport dynamics on the continental shelf and in estuaries and developing instrumentation to measure these processes.

Dr. Traykovski is a member of the American Geophysical Union.

Peter A. Howd received the M.S. and Ph.D. degrees in oceanography from the Oregon State University, Corvallis, in 1984 and 1991, respectively.

Currently, he is an Oceanographer at the U.S. Geological Survey (USGS) Center for Coastal and Watershed Studies, St. Petersburg, FL. His research focuses on understanding the longshore variability of both fluid processes and morphologic responses during extreme storm events on beaches and barrier islands. Before joining the USGS, he taught at the Duke University Marine Laboratory and at the University of South Florida. He was also an Oceanographer at the U.S. Army Corps of Engineers, Field Research Facility.

Dr. Howd is a member of the American Geophysical Union.

Paul A. Elmore received the B.S. degree in physics from the Millsaps College, Jackson, MS, in 1990 and the Ph.D. degree in physics from the University of Mississippi, Oxford, MS, in 1996.

He received a fellowship from the American Society of Engineering Education to pursue postdoctoral research in ocean acoustics in the Acoustics Division of the Naval Research Laboratory (NRL), Stennis Space Center, MS, from 1996 to 1998. Then, he worked for the U.S. Navy as a Physicist at the Naval Oceanographic Office, Stennis Space Center, MS, from 1998 to 2001. Since 2001, he has been a Research Physicist for the Marine Geosciences Division of the NRL. His research interests are in nonlinear acoustics, ocean acoustics, seafloor sensing, and nearshore environmental prediction.

Dr. Elmore is a member of the American Geophysical Union. He was a Graduate Fellow at the National Center for Physical Acoustics, the University of Mississippi.

Thomas F. Wever received the Diploma degree in geophysics and the Ph.D. degree in field of continental crustal studies using reflection seismic methods, both from the Christian-Albrechts-Universität, Kiel, Germany, in 1985 and 1988, respectively.

He spent two months with PRAKLA-SEISMOS (now part of Schlumberger), Hannover, Germany, during his studies at the university and three semesters at Ludwig-Maximilians-Universität, Munich, Germany. Since 1990, he has been a Research Scientists at the Forschungsanstalt der Bundeswehr für Wasserschall und Geophysik (FWG), Kiel, Germany. He started in the field of sonar range prediction and, since 1992, has been working in the field of mine burial prediction and seafloor studies.

Dr. Wever is a member of the American Geophysical Union (AGU) and the European Association of Geoscientists and Engineers (EAGE).